Effect of niobium on the directional solidification and properties of Alnico alloys

S. PRAMANIK, V. RAO, O. N. MOHANTY
National Metallurgical Laboratory, Jamshedpur 831 007, India

The effect of niobium on the extent of columnar growth of grains and on the magnetic properties in Alnico alloys has been studied. Alloys containing 1% Nb show maximum growth of columnar crystals. In columnar alloys, coercivity increases slowly with increasing niobium content up to ~ 1%. With further increase in niobium, coercivity and remanence decrease. The maximum energy product (55 kJ m^{-3}) has been obtained at 1% Nb. Niobium addition has also been found to suppress the precipitation of the undesirable γ phase.

1. Introduction

Considerable work has been reported in the literature on Alnico alloys [1–6]. Alnico V which contains 8% Al, 14% Ni, 24% Co, 3% Cu and balance Fe, is known to give rise to a maximum energy product [$(BH)_{max}$] of 40–44 kJ m^{-3}. Further improvement in properties is possible through directional solidification. Directionally solidified Alnico alloys have grains parallel to the $\langle 100 \rangle$ direction resulting in higher remanence (1.3–1.4 T), good coercivity (55–66 kA m^{-1}) and a $(BH)_{max}$ of 50–70 kJ m^{-3}. Recent studies [7–10] have shown that the properties of directionally solidified Alnico alloys can further be improved by addition of small amounts of niobium. A systematic study, however, on the effect of niobium on the extent of columnar crystallization and magnetic properties, has not been reported in the literature.

The present work pertains to the studies carried out on the effect of niobium (0–2 wt%) on columnar crystallization and magnetic properties in Alnico V alloys.

2. Experimental procedure

Five alloys were made. Low-carbon iron, cobalt, electrolytic copper and nickel were melted in a 2 kg induction furnace and then electrolytic aluminium was added. After deoxidizing with small amounts of silicon, the melt was held in the furnace for 2 min. Subsequently, niobium was added in the form of ferroniobium. Molten metal was then poured into a specially made refractory mould (Fig. 1).

Moulds were made from 4 in (10 cm) diameter refractory sleeves and 1 in (2.5 cm) diameter sillimanite tubes which were fixed at the centre of the sleeves (using sand and sodium silicate). The sillimanite tube helped in obtaining castings with smooth surfaces, thereby avoiding columnar growth of crystals from the walls of the mould. The moulds were heated to 1000 °C and placed on a water-cooled copper plate.
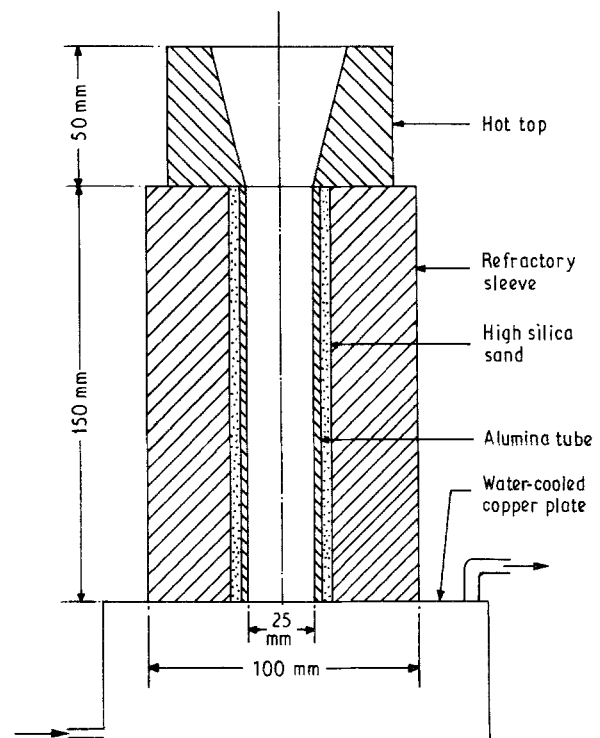

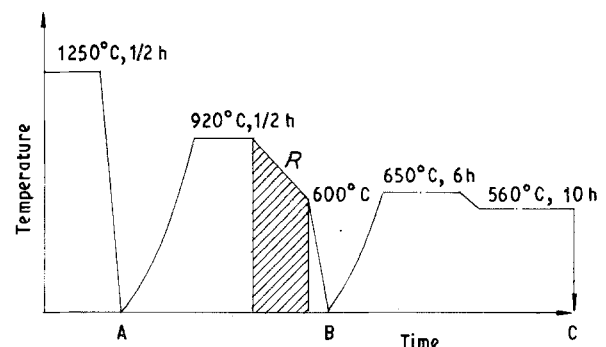*Figure 1* Schematic diagram showing the mould arrangements for directional solidification.

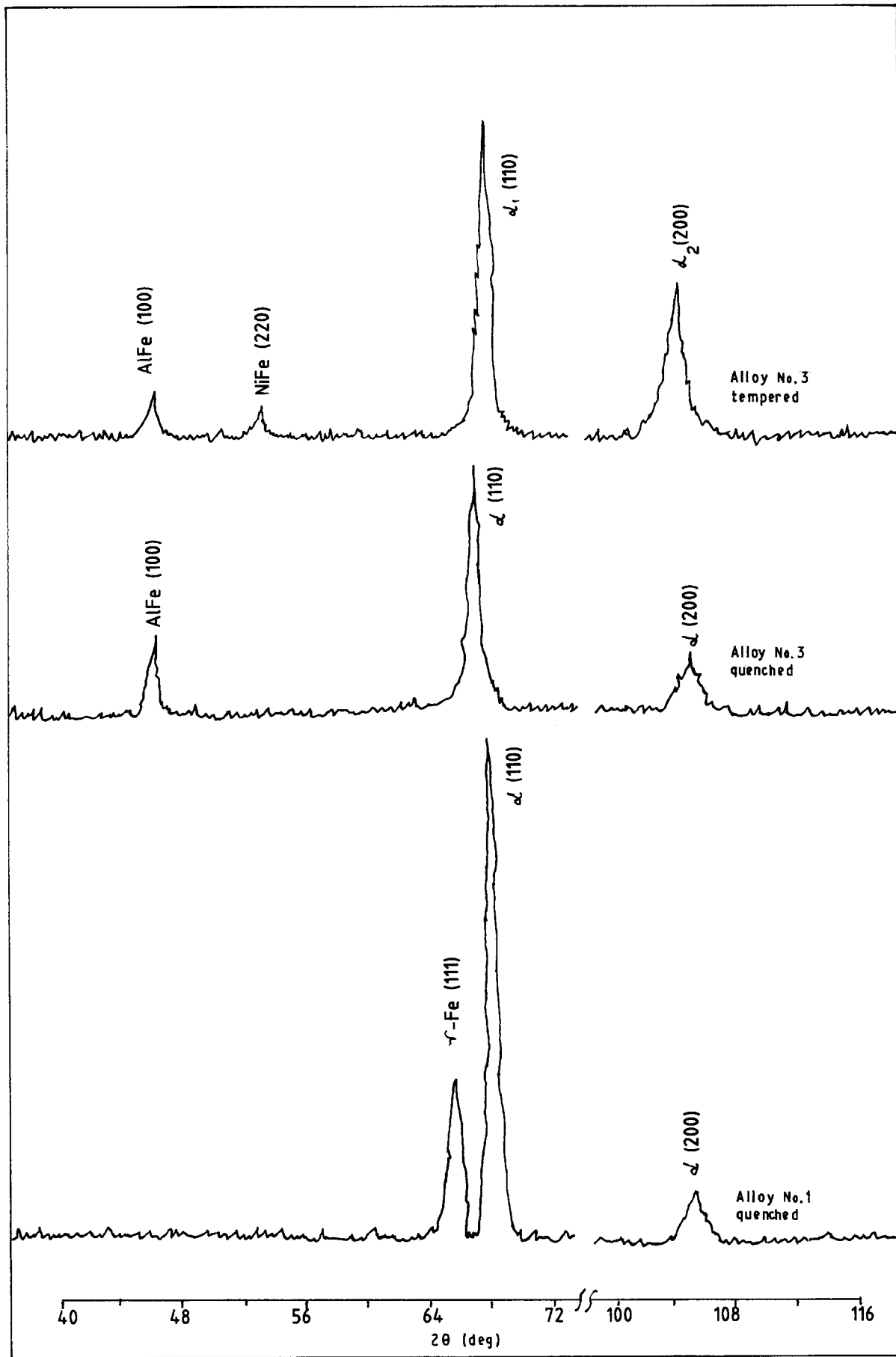*Figure 2* Schematic diagram of heat-treatment schedule. R = 32 °C min^{-1} in a magnetic field.

Figure 3 X-ray diffraction patterns of quenched and tempered Alnico alloys.

Alloy	Al	Ni	Co	Cu	Nb
1	8	14	24	3	–
2	8	14	24	3	0.5
3	8	14	24	3	1.0
4	8	14	24	3	1.5
5	8	14	24	3	2.0

The metal was then poured at a temperature of 1650 °C and exothermic mixture was added on the hot top placed over the heated mould.

Specimens 10–20 mm thick were cut from the bottom as well as the upper portions of each ingot for heat treatment and magnetic measurements. All the specimens were homogenized at a temperature of 1250 °C for 30 min and cooled in a blast of air. The specimens were cooled at the rate of $0.5\,°C\,s^{-1}$ from 920–600 °C in a magnetic field of $20\,kA\,m^{-1}$, then cooled to room temperature without the magnetic field. The specimens were tempered first at 650 °C for 6 h and finally at 560 °C for 10 h. A schematic representation of the heat-treatment schedule is given in Fig. 2.

To study the extent of columnar growth of crystals, 2 in (5 cm) long samples were cut from the bottom portion of each ingot and sectioned longitudinally into two halves. The inside surface was macro-etched with an etching solution containing 5 g cupric chloride, 1 g stannous chloride and 10 g ferric chloride dissolved in 100 ml HCl and made up to 500 ml with water.

For X-ray diffraction studies, 5 mm thick specimens from the bottom portion of each ingot were used. X-ray diffractograms were taken on Siemens X-ray diffractometer, model D-500 using CrK_{α} radiation. X-ray and metallographic studies were made in the as-cast, air-quenched and double-tempered conditions.
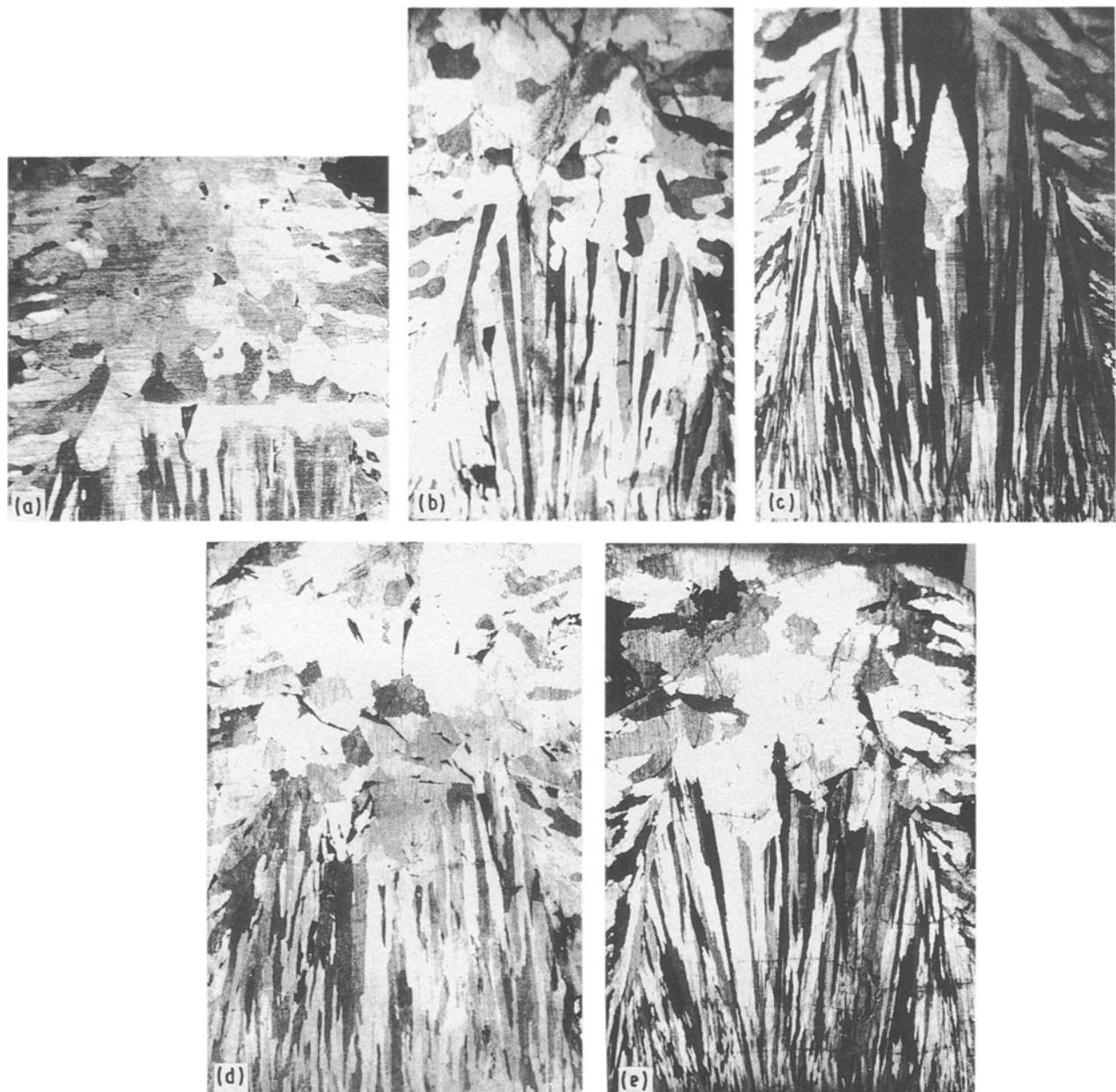

Figure 4 Macrostructures of columnar Alnico alloys in as-cast conditions. Alloy: (a) 1, (b) 2, (c) 3, (d) 4, (e) 5.

For TEM studies, a standard carbon extraction replica technique was used for samples in the heat-treated condition.

The magnetic measurements were made using Walker's Hysteresisgraph, model MH-3020. The samples for measurement were taken from the central portion of the columnar regions where the grains were nearly parallel.

3. Results and discussion

Table I gives the nominal composition of the alloys studied. Alloy 1 corresponds to the conventional Alnico V, and the others contain varying amounts of niobium.

X-ray diffraction patterns of a few quenched and tempered alloys are shown in Fig. 3.

The macrostructures of the cast alloys (Fig. 4) reveal that (a) columnar crystals are quite thick and (b) the length of the columnar crystals formed is maximum when the niobium content is 1%. Fig. 5a shows the microstructure of Alloy 1 containing no niobium, cooled in blast of air from 1250 °C. The structure shows predominantly single phase (α) with some precipitation of a second phase (probably γ phase). X-ray diffraction studies have also shown the presence of γ

phase. Fig 5b shows the microstructure of the same alloy in the fully tempered condition. The structure shows the presence of α_1 and α_2 phases with some γ phase as indicated by X-ray diffraction data. Fig. 6a and b show the microstructures of Alloy 3 (containing 1% Nb) in the air-quenched condition, the top (equiaxed) and bottom (columnar) portions of the ingot, respectively. As can be seen, in both the cases, there is no precipitation of γ phase, as evinced by XRD studies.

Scanning electron micrographs of Alloy 3 are shown in Fig. 7. The aspect ratio of α_1 particles in the spinodally aged columnar alloy appears to be much larger than that of the equiaxed alloy (Fig. 7c and d). TEM features of Alloy 1 are shown in Fig. 8. Whereas the SAD pattern of the alloy containing no niobium (Alloy 1) (Fig. 8b) shows the presence of γ phase, the alloy containing niobium (Alloy 3) has no γ phase [11]. Table II gives the magnetic properties of the columnar samples from different alloys in the spinodally aged condition. This table shows that the desirable magnetic properties are not yet developed at this stage (Stage B). Alloy 1, though, has exhibited high coercivity, H_c, has shown a lower remanence, B_r, compared to Alloy 3. Table III and Figs 9 and 10 depict the magnetic properties of the alloys after final
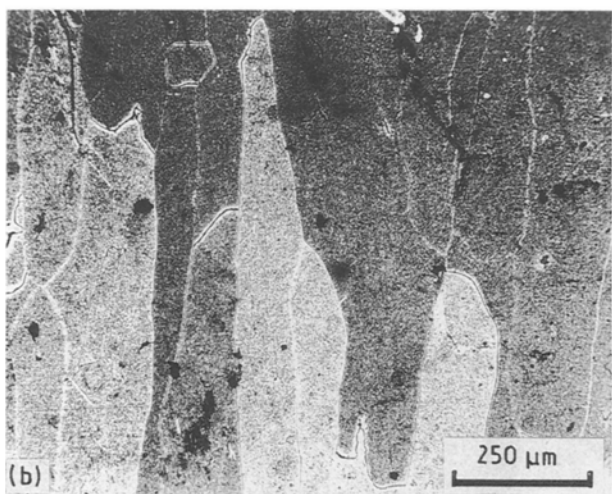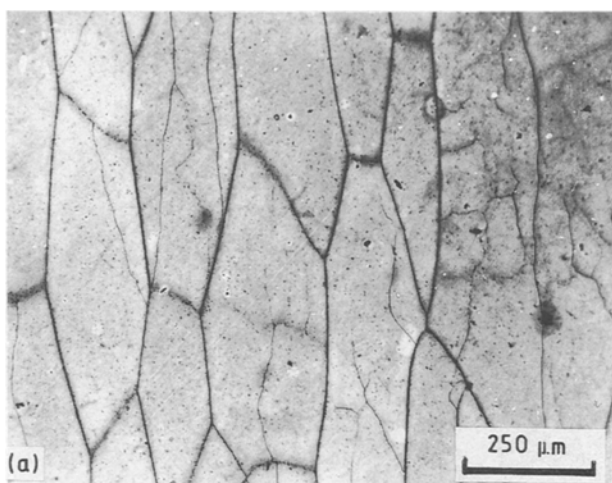

Figure 5 Microstructures of columnar alloy containing no niobium (Alloy 1), (a) quenched in blast of air and (b) tempered.
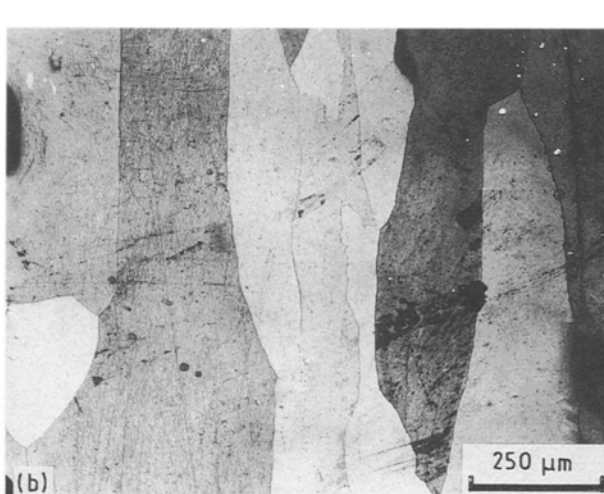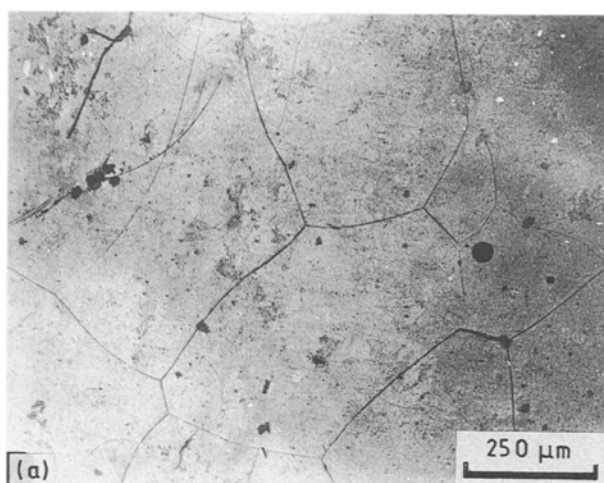

Figure 6 Microstructures of quenched niobium-containing alloy (Alloy 3), (a) equiaxed, (b) columnar.
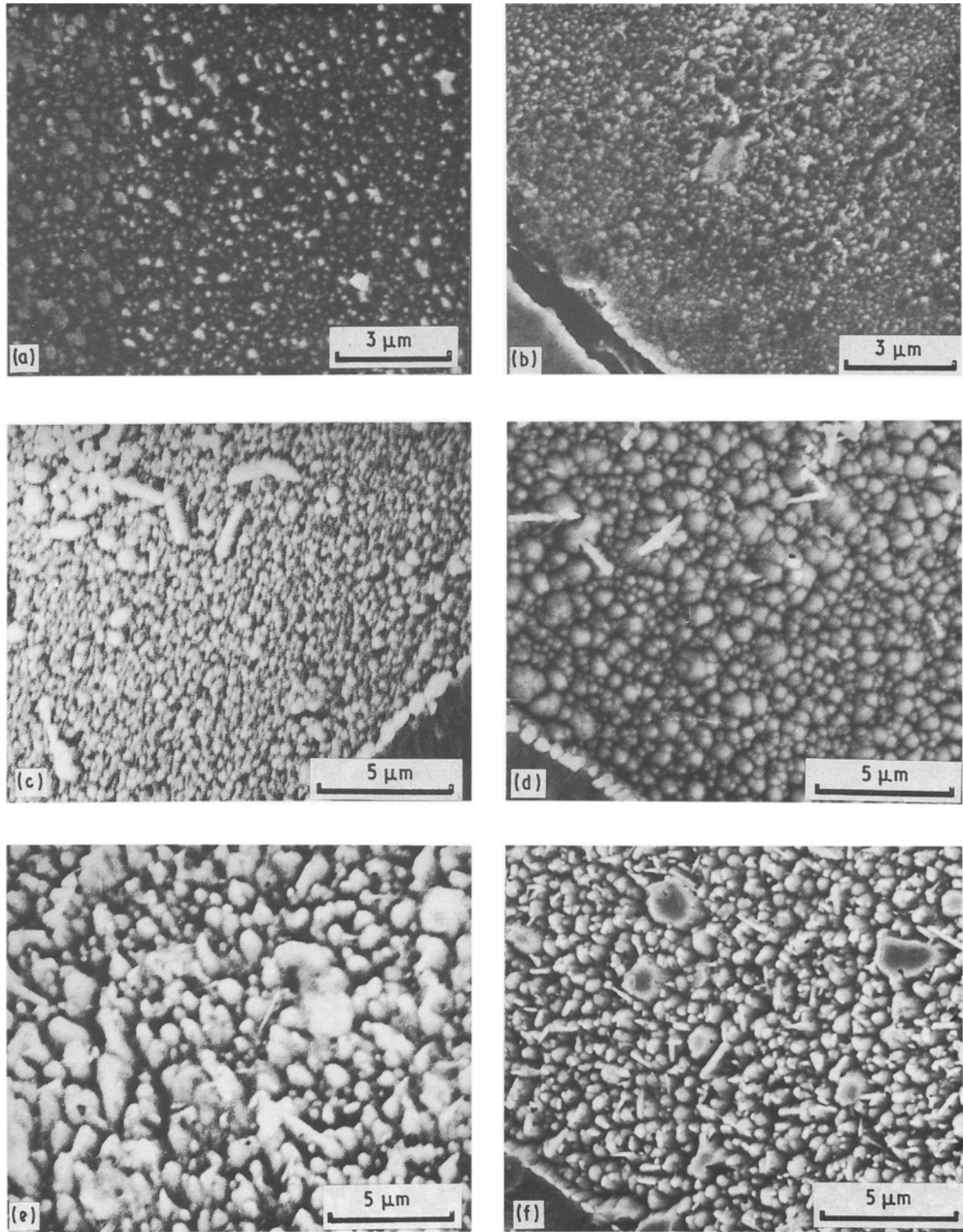
1240

Figure 7 Scanning electron micrographs of Alloy 3: (a, c, e) columnar and (b, d, f) equiaxed. (a, b) Homogenized, (c, d) cooled under a magnetic field, (e, f) tempered.

heat treatment (Stage C of Fig. 3). These figures also describe the influence of niobium on the magnetic properties in the equiaxed (Fig. 9) as well as columnar regions (Fig. 10). It is evident, when one compares these with the magnetic properties obtained at Stage B, that there is an appreciable improvement after going through Stage C. From Fig. 9 it can be seen that the

remanence, B_r, and energy product, $(BH)_{max}$, values of equiaxed alloys decrease continuously with the addition of niobium. Coercivity, H_c, remains constant up to 1.5% Nb and then decreases. The decrease in remanence and hence $(BH)_{max}$ is attributed to the dilution effect of non-magnetic niobium addition which decreases the saturation induction and hence B_r [12].
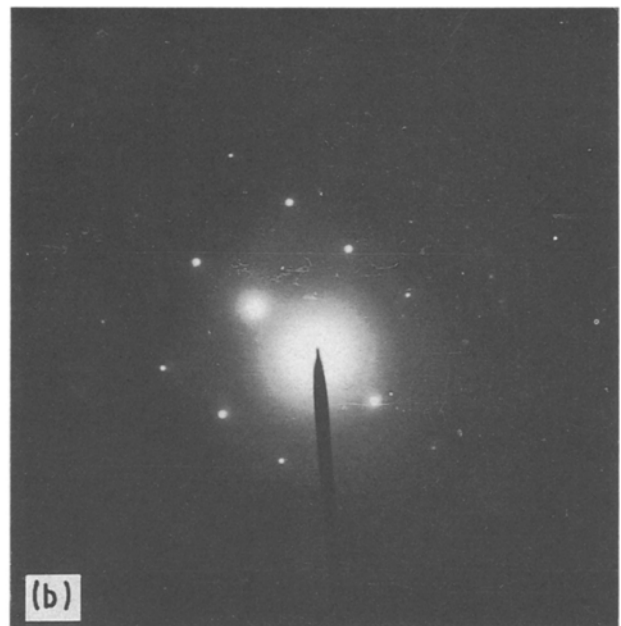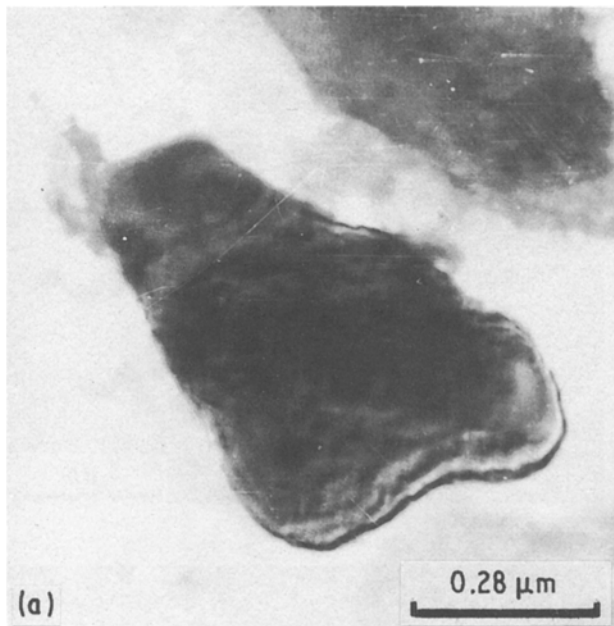
Figure 8 (a) Transmission electron micrograph (replica) of Alloy 1, air quenched. (b) The corresponding SAD pattern and indexing.

(331)

(311)

(020)   (331)

(000)

(b)

TABLE II Magnetic properties of columnar Alnico alloys after spinodal ageing (Stage B, Fig. 2)

Alloy	H_c(kA m^{-1})	B_r(T)	$(BH)_{max}$(kJ m^{-3})
1	33.0	1.0	12.48
2	20.4	1.13	8.96
3	12.3	1.04	4.88
4	26.6	1.0	8.88
5	8.8	0.76	2.48

Beyond 1.5% Nb, the particles are probably of multi-domain size, thus reducing the coercive force.

In the columnar specimens (Fig. 10) it may be seen that remanence continuously, but only marginally, decreases from 1.3 T to 1.27 T with the addition of niobium up to 2%, as expected, due to the dilution effect of niobium [10]. The remanence values of columnar samples have been found to be much higher than those of the equiaxed ones. The higher values of remanence in columnar alloys may be ascribed to better alignment and distribution of the ferromagnetic α_1 phase in a feebly magnetic matrix of α_2 phase. The coercivity of columnar alloys is, in general, higher than that of corresponding equiaxed ones. This is attributed to the shape anisotropy of the columnar
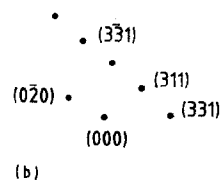
alloys. The coercivity in columnar alloys was found to increase with increasing niobium content and is maximum at 1% Nb (Fig. 10) [10]. Beyond this point, H_c decreases. The maximum H_c at 1% Nb may be due to the reduction in number of domains in the α_1 phase. Dispersion of the ferromagnetic α_1 phase in the matrix of α_2 phase reduces the demagnetizing field and hence the increase in the coercive force. The adverse effect of niobium beyond 1% is probably due to the formation of multidomain α_1 particles. As the H_c is maximum and the remanence more or less constant at 1% Nb, one would expect the highest value of $(BH)_{max}$ at 1% Nb. The maximum value in $(BH)_{max}$, in fact, has been observed at 1% Nb (Fig. 10). Some detailed characteristics of the alloy containing 1% Nb (Alloy 3) will now be discussed. Fig. 11 shows the demagnetization and energy product behaviour for Alloy 3. The shape of the demagnetization curve shows that the anisotropy has been achieved to the desirable extent, taking into account the fact that the coercive force and the remanence obtained in the alloy are both reasonably high. From the XRD one finds mostly the presence of α phase, with some intermetallics such as

TABLE III Magnetic properties of Alnico alloys after final tempering (Stage C of Fig. 2)

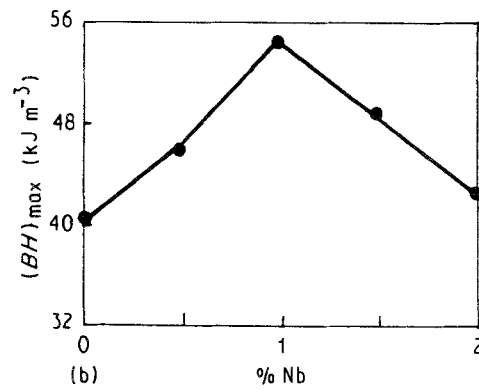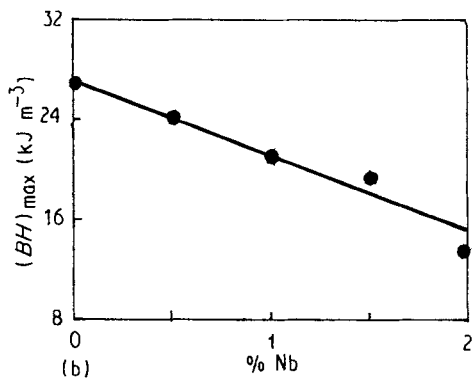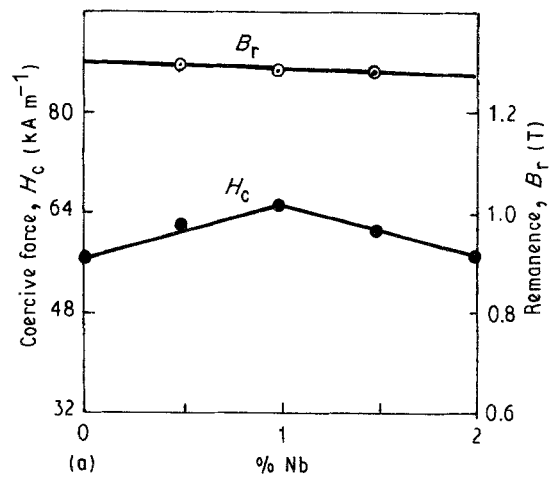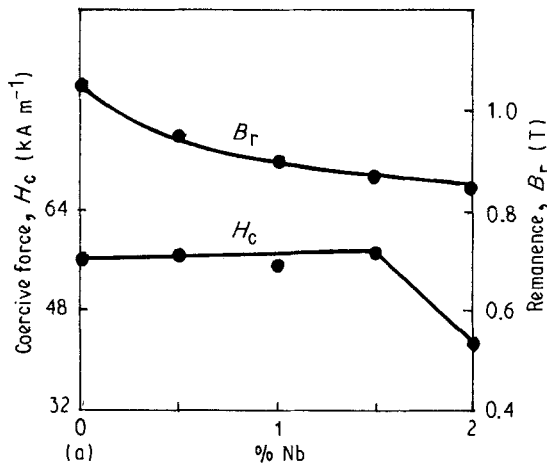| Alloy	Equiaxed			Columnar		
	H_c (kA m^{-1})	B_r (T)	$(BH)_{max}$ (kJ m^{-3})	H_c (kA m^{-1})	B_r (T)	$(BH)_{max}$ (kA m^{-3})
1	56.5	1.05	26.96	55.7	1.3	40.0
2	56.5	0.95	24.0	61.3	1.29	46.0
3	55.3	0.90	20.72	64.5	1.28	55.0
4	57.3	0.88	19.36	60.5	1.28	48.0
5	42.2	0.85	13.52	56.5	1.27	42.0

Figure 9 Effect of niobium on the magnetic properties of equiaxed alloys.

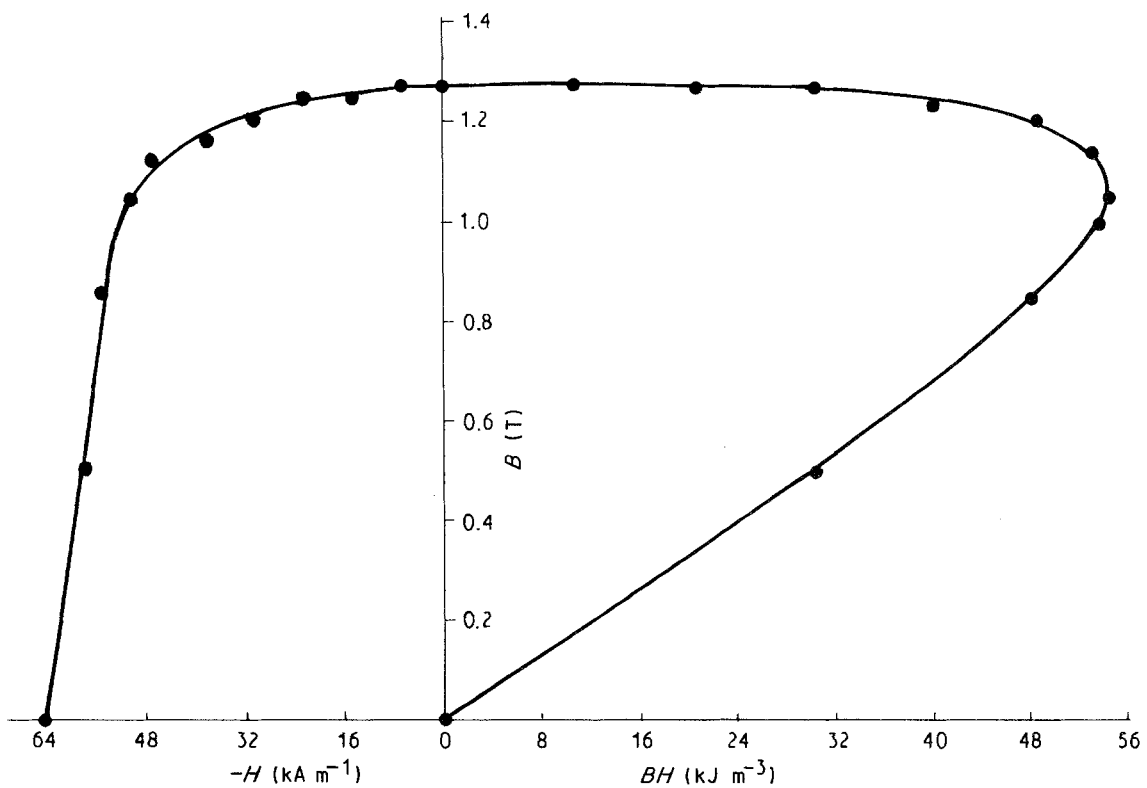*Figure 10* Effect of niobium on the magnetic properties of columnar alloys.

Figure 11 Demagnetization and energy product curves of alloy 3 (columnar) after final tempering.

NiFe in the as-cast as well as Stage A (Fig. 3) conditions. However, after Stage C, one observes primarily α_1 and α_2 phases. Further improvement in the magnetic properties, i.e. $(BH)_{max}$, can only be expected through either improvement in H_c (by addition of elements like titanium) or improvement in remanence (through better alignment of the columnar grains) or both.

4. Conclusions

1. Niobium addition prevents the precipitation of undesirable γ phase.

2. The length of the columnar crystals is maximum at 1% Nb. More than 1% Nb addition decreases the length of the crystals.

3. Remanence decreases with addition of niobium.

4. Coercive force increases with increase in niobium content and at 1% Nb it reaches a maximum. Further addition of niobium decreases the coercive force.

5. The energy product is maximum at 1% Nb.

References

1. M. McCAIG, *Proc. Phys. Soc.* **B62**, (1949) 652.
2. K. J. De VOS "Alnico Permanent Magnet Alloys", in "Magnetism and Metallurgy", Vol. 1 (Academic Press, New York, London, 1969) pp. 473–512.
3. C. D. GRAHAM Jr, "Textured Magnetic Materials", in "Magnetism and Metallurgy", Vol. 2 (Academic Press, New York, London, 1969) pp. 723–48.
4. J. E. GOULD *Proc. Inst. Elec. Eng.* **106A** (1959) 493.
5. *Idem, Cobalt* **23** (1964) 82.
6. ANON, *ibid.* **18** (1963) 26.
7. A. I. LUTEIJN and K. J. de VOS, *Phil. Res. Rep.* **11** (1956) 489.
8. W. S. MESAKIN and B. E. SOMIN *Archiv Eisen.* **8** (1934) 315.
9. A. J. BRADLEY and A. TAYLOR, *Proc. Roy. Soc.* **166A** (1938) 353.
10. S. SZYMURA and S. GOLBA *J. Magn. & Magn. Mater.* **24** (1981) 285.
11. SHI MING HAO, K. ISHIDA and T. NISHIZAWA, *Met Trans.* **A16** (1985) 179.
12. C. BRONNER, J. P. HABERER, E. PLANCHARD and J. SAUZE, *Cobalt* **46** (1970) 15.